SAR Image Processing Applications with Target Preservation

Fátima N. S. Medeiros, Regis C. P. Marques, Daniela M. Ushizima and Charles I. O. Martins
Federal University of Ceará - DETI/UFC, Fortaleza, CE, Brazil

***Abstract*—This paper presents algorithms for synthetic aperture radar (SAR) image processing with target preservation. SAR images are corrupted by speckle noise that degrades the performance of processing algorithms applied to these images. In several applications the speckle noise is reduced by filtering algorithms, however this process can smear image details as punctual targets. We approach image processing techniques developed to deal with target preservation in three distinct applications: segmentation, compression and filtering. The algorithms were validated by tests on synthetic and real SAR images and the results indicate that they constitute well-accepted approaches to support SAR image processing with target preservation.**

***Index Terms*—Active and passive sensors, SAR, target processing.**

I. Introduction

Targets can be detected from SAR images when an area of few resolution cells presents distinguishable properties from the clutter, usually indicating that this local area is too bright [1]. This task is challenging due to the speckle phenomena and the inaccuracy of traditional algorithms in processing SAR images corrupted by such a noise. Most of the algorithms propose pre-processing steps to filter speckle noise, which are decoupled to the application, often degrading fine details and edges that would be valuable for detection and compression steps.

Attempting to solve these drawbacks we present three frameworks for SAR image processing, reviewing their advantages regarding target preservation in three distinct applications. The first approach, as proposed in [2], detects target by including speckle statistics [3] in the front propagation model to enclose small or point targets and fine details in L-looks amplitude SAR images. It is based on a level set [4] evolution model to address the front movement according to speckle statistics. Hence it incorporates a local neighborhood homogeneity measure and an adaptive windowing scheme [5] to achieve target detection in speckled images.

Our second approach was exposed in [6] and it consists of a compression framework that tracks regions with targets in a bounded variation image [7] to employ a lossless compression method to these regions with the purpose of preserving targets. The adaptive compression scheme is a modified version of the well known SPIHT method [8] named in this paper as MSPIHT.

The filtering scheme presented in [9] combines the self-dual reconstruction [10] and the Lee [11] and alternating sequential [10] filters. The classical self-dual filter uses the median filter to obtain marker images for the filtering process. Our approach applies the Lee filter to generate marker images. The major contribution of this filtering algorithm is to be fairly insensitive to the choice of the window size in comparison with the Lee filter. In addition, we can easily modify the proposed scheme to include other standard speckle filters (e.g. Frost and Kuan) to generate marker images.

This paper is organized as follows: We present in Section II the method for SAR segmentation and in Section III the one that approaches SAR image compression with the aim of preserving targets. The speckle filtering algorithm is presented in Section IV. Finally, Section V concludes this paper and presents further works that can be investigated.

II. Small target detection driven by speckle statistics

The method for target detection proposed in [2] is based on statistics of speckle into homogeneous regions. Speckle is a noise always associated with coherent-illuminated scenes and signal degradation is described in accordance with the multiplicative model. The SAR system return X is given by $X = YZ$, with the speckle noise Z and radar cross-section Y assumed statistically independents.

Let $\mathbf{x}$ be a pixel in a SAR image X ($\mathbf{x} \in X$) and W_M a MxM sliding window centered in $\mathbf{x}$, then the homogeneity measure presented in [5] can be estimated in the $\mathbf{x}$ neighborhood as the standard deviation to mean ratio. This measure is a sample estimate of speckle noise standard deviation σ_z.

The adaptive scheme consists in changing the window size M, automatically, while the pixel neighborhood is heterogeneous, a decision taken by comparing the speckle standard deviation (σ_z) to the theoretical variation coefficient given by:

$$C_z = \frac{0.5227}{\sqrt{\text{Number of Looks}}} \tag{1}$$

with a threshold T, namely

$$T = 1 + \frac{\sqrt{1 + 2{C_z}^2}}{\sqrt{2M^2}} C_z \tag{2}$$

The parameter T is an estimate of C_z, defined as a threshold for the local homogeneity, which controls the window size

F. N. S. Medeiros, fsombra@ufc.br, GPI - Image Processing Research Group, Teleinformatics Department, Federal University of Ceará - DETI/UFC, Fortaleza, CE, Brazil.
R. C. P. Marques, regismarques@ifce.edu.br, Federal Institute of Education, Science and Technology (IFCe), Fortaleza, CE, Brazil.
D. M. Ushizima, dusjizima@lbl.gov, Math and Visualization Groups, Lawrence Berkeley National Laboratory (LNBL), Berkeley, CA, USA.
C. I. O. Martins, charlesiury@gmail.com, Vision - IME, University of São Paulo, SP, Brazil.

decrease or increase. The goal is to obtain the optimum window size for local processing applications for image filtering improvement [5].

The estimated homogeneity of the terrain reflectivity is more accurate for larger windows due to the number of boundary samples. Assuming that σ_z is a sample estimate, we can measure the σ_z variation around the theoretical value.

Since the optimal window size is defined, the region fluctuations close to the classification threshold T can be measured by $T-\sigma_z$, thereby $T-\sigma_z > 0$ for non-homogeneous regions and $T-\sigma_z < 0$ for homogeneous ones. These fluctuations can be well tractable as a propagation model, which one leads to convergence along the boundary $T-\sigma_z \approx 0$.

The central idea in the level set methods is to represent a front $\gamma(t)$ as the initial level $\psi(\mathbf{x},t)=0$ of a surface $\psi(\mathbf{x},\mathbf{t})$, where $\mathbf{x} \in \Re^n$ [4]. The goal is to produce a front motion as consequence of the surface motion, in which $\gamma(t)$ is embedded in accordance to:

$$\gamma(t)_{t=0} = (\mathbf{x}|\psi(\mathbf{x},t)=0)_{t=0} \tag{3}$$

where

$$\psi_{n+1} = \psi_n + \Delta t \; F|\nabla\psi_n| \tag{4}$$

and

$$F = -((T-\sigma_z)+\varepsilon K)\vec{n} \tag{5}$$

The term εK in Eq.(5) is the curvature speed [4].

Fig. 1 illustrates the processing steps of the proposed algorithm applied to a synthetic image, which was artificially contaminated with 6-looks speckle statistics, as depicted in Fig. 1(a). Inspired by [12], we have used a set of fronts to start the method. Fig. 1(b) shows the starting process, i.e the initial level set stage. An intermediary stage of the front propagation is depicted in Fig. 1(c) and Fig. 1(d) illustrates the final image result.

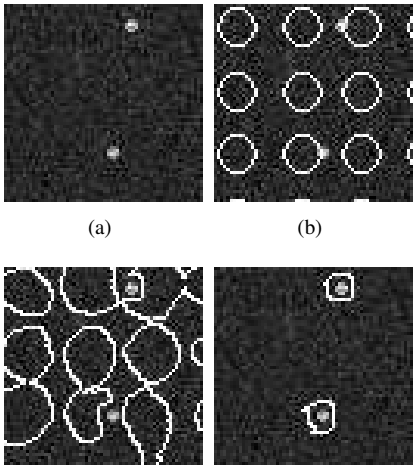

Fig. 1. Level set evolution according to speckle statistics: (a) Synthetic image with 6-looks speckle statistics, (b) initial level set stage, (c) intermediary stage and (d) the final result.

Fig. 2 displays a RADARSAT 4 looks image over the coastal zone in RN-Brazil. The sample size is 512x512 pixels and it shows offshore oil platforms. One can observe that our method succeeded in locating the small bright targets (oil platforms).

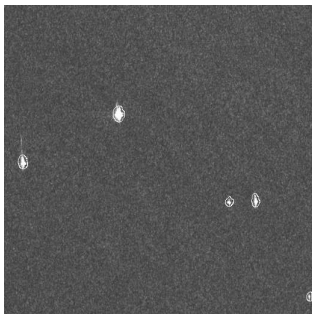

Fig. 2. Segmentation result of the proposed algorithm applied to a real 4-looks SAR image (512 x 512 pixels) containing offshore oil platforms.

III. SAR Image Compression with Target Preservation

This paper approaches image compression with target preservation as an adaptive bit rate compression scheme regarding previous target neighborhood identification [6]. The compression algorithm decomposes SAR images into BV and L^2 spaces [13]. This algorithm encloses two components: u, with the low frequency information and v, with the high frequency information; these components are associated to the BV and L^2 spaces, respectively, and provide image analysis using distinct bands in the same resolution. Similar to [7], the proposed scheme employs the Total Variation Minimization (TV) method to obtain the u component. The oscillating component v can be computed as a TV residual information.

To perform target detection, the u component is subdivided into blocks according to a proposed criterion by using the quadtree decomposition [14]. If a block meets this proposed criterion, it is not subdivided, otherwise it is decomposed into four blocks. The criterion is defined as $\sigma_L < \sqrt{L}(\sigma_{L-1})$, where L is the quadtree decomposition level and σ_L is the standard deviation of the inspected block.

Our aim is to allocate more bits in the compression process to fine details scales. Hence in the highest decomposition scale (16x16 blocks) we apply the arithmetic coder to provide a lossless data compression. The other scales (32x32, 64x64,128x128) are compressed by applying the SPIHT algorithm [8] with decreasing bit rates.

Fig. 3(a) displays a scene of the coastal zone in RN-Brazil. The image size is 256x256 pixels with 12.5 m resolution. It was acquired in amplitude detection from the RADARSAT system. The decomposition (BV) result can be observed in Fig. 3(b) which illustrates the preserved targets, bright points in the top center and an oil slick down center in the u component. The quadtree decomposition provides a partition (grid) displayed in Fig. 3(c). It can be observed in Fig. 3(d) bright targets in fine scales (16x16 and 32x32 blocks) and the oil slick divided into 64x64 blocks.

The quantitative measures used to assess the experimental results were **PSNR** (Peak Signal to Noise Ratio) and standard

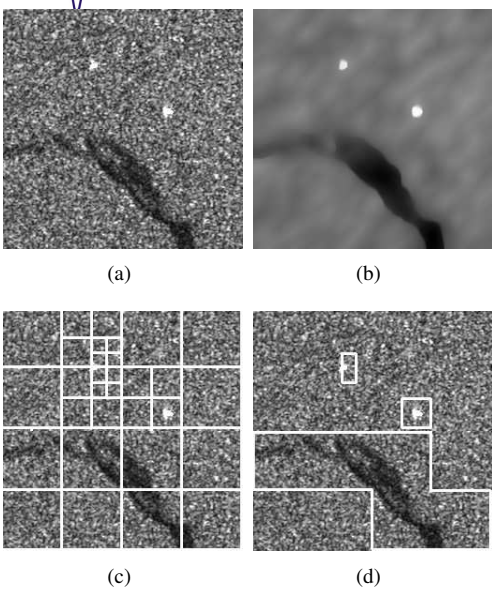

Fig. 3. (a) The original SAR image, (b) the u component, (c) the quadtree decomposition (grid) superimposed in the original image and (d) the detected targets.

deviation to mean ratio σ_m[14]. In addition, the **MIE** (Max Intensity Error) [15] was locally computed as a measure of fine details preservation. The modified SPIHT (MSPIHT) outperformed the standard JPEG2000 compression method according to the assessment measures. Furthermore, it was superior to the conventional SPIHT method related to MIE and σ_m measures.

Table I shows the evaluation of the algorithm performance for two different bit rates, 0.2 bpp and 1.0 bpp. One can observe that the proposed method presented similar PSNR values as SPIHT with a reduction of 0.5 dB.

TABLE I
ASSESSMENT MEASURES

Bit Rate		0.2 bpp	1.0 bpp
MSPIHT	PSNR(dB)	31.47	37.47
	MIE(dB)	12.30	7.780
	σ_m	0.194	0.277
SPIHT	PSNR(dB)	31.50	38.02
	MIE(dB)	13.80	10.41
	σ_m	0.166	0.231
JPEG2000	PSNR(dB)	31.13	37.34
	MIE(dB)	17.50	10.00
	σ_m	0.154	0.274
Original Image	$\sigma_m = 0.278$		

IV. ITERATIVE SELF-DUAL RECONSTRUCTION FOR SAR IMAGE ENHANCEMENT

Morphological reconstruction by dilation (or erosion) is an operator that removes dark (or bright) regions from a marker image constrained by a mask image. Particularly, self-dual reconstruction combines reconstruction using dilation and erosion to achieve the same treatment to dark and bright regions of the image. The self-dual reconstruction $R_g^{\nu'}(f)$ of a marker image f constrained by a mask image g is defined by [10]:

$$[R_g^{\nu'}(f)](\mathrm{x}) = \begin{cases} [R_g^{\delta}(f \wedge g)](\mathrm{x}), \text{ if } f(\mathrm{x}) \leq g(\mathrm{x}). \\ [R_g^{\varepsilon}(f \vee g)](\mathrm{x}), \text{ otherwise} \end{cases} \quad (6)$$

where R^{δ} and R^{ε} correspond to the morphological reconstruction by dilation and erosion, respectively.

Our method adapts the Lee filter with morphological reconstruction by performing adequate noise removal with image statistics, and maintaining fine image details. We propose that the window size increases in each iteration according to the relation: $W_n = W_1 + 2 \times (n-1)$, where W_1 and n ($n \geq 1$) relate to the minimum window size (3x3) and the number of the current iteration, respectively. Thus, the second iteration generates a Lee filtered marker image with a 5×5 window (W_2), the third with a 7×7 window (W_3), the fourth with a 9×9 window (W_4) and so on.

The implemented algorithm denoted Iterative Reconstruction from Lee ($IRLee$) filter of order n is described as follows:

$$IRLee_n(f) = \begin{cases} R_{L_1(f)}(f), \text{ for } n = 1 \\ R_{L_{n-1}(IRLee n_1(f))}(f), \text{ for } n > 1 \end{cases} \quad (7)$$

where $L_n(f)$ denotes the Lee filter applied to an image f using a window of size W_n.

The $IRLee$ filtering starts by considering the $IRLee_0$ image to be the original one (speckled image), then the Lee filter is applied to the $IRLee_{n-1}$ image, generating a marker image L_n and the final $IRLee_n$ image is obtained by the reconstruction process using the original image as a mask. Here, instead of estimating the standard deviation of the speckle noise (σ_n) in each $IRLee$ image we keep it constant for every iteration. We assume that some pixel values in each iteration are still affected by the multiplicative noise and therefore we can use the same σ_n parameter for the Lee filter with a larger window. This assumption is motivated by the self-dual reconstruction filter effect obtained when it is applied to the previous Lee filtered image. The self-dual reconstruction filter modifies several pixel values turning them into values closer to the related ones in the mask image.

To evaluate edge preservation in filtering process, we have used the A coefficient [16], [17]. It is described as

$$A = \frac{\Gamma(\Delta S - \overline{\Delta S}, \widehat{\Delta S} - \overline{\widehat{\Delta S}})}{\sqrt{\Gamma(\Delta S - \overline{\Delta S}, \Delta S - \overline{\Delta S}).\Gamma(\widehat{\Delta S} - \overline{\widehat{\Delta S}}, \widehat{\Delta S} - \overline{\widehat{\Delta S}})}} \quad (8)$$

where ΔS and $\widehat{\Delta S}$ are the high-pass filtered versions of an original image (S) and the denoised one ($\hat{S}$), respectively, obtained with a 3×3 pixel standard approximation of the Laplacian operator and the function $\Gamma(S_1, S_2) = \sum_{i=1}^{K} S_{1i}.S_{2i}$ [9].

Fig. 4(d) displays the A values calculated for the processed images using the Lee and $IRLee$ filters over the filtered versions of the noisy image in Fig. 4(a). In Fig. 4(d), the curve of A values for the Lee filter shows that the edges are not preserved (A tends to values close to zero) as the window's

size increases. This is an evidence that the use of the Lee filter with an analyzing window with dimensions greater than 5×5 does not guarantee edge preservation. This effect is not observed for the $IRLee$ filter in the same graphic, where the A values asymptotically approximates A=0.22 as the number of iterations of the proposed algorithm increases.

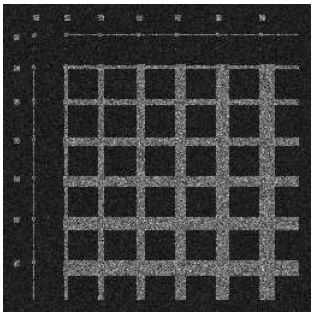

(a)

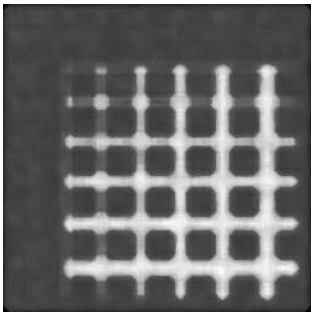

(b)

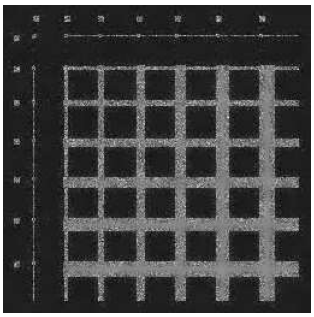

(c)

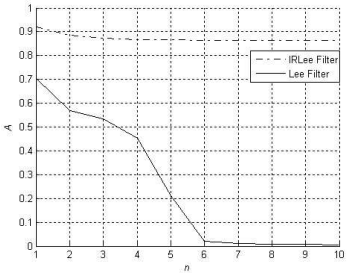

(d)

Fig. 4. (a) Simulated 3 looks SAR image, (b) blurring effect observed for $n = 5$ by applying the median filter, (c) the Lee filter to obtain the mask images for the $IRLee$ filter and (d) A values calculated to images processed by the Lee filter using an window of increasing size (solid) and processed by $IRLee$ filter with an increasing amount of iterations (dashed).

Though the number of looks should, in principle, be an integer, seldom this is the case when this quantity is estimated from real data due to, among other reasons, the fact that the mean is taken over correlated observations. It is therefore interesting to call the equivalent number of looks;

Fig. 5 shows the filtering result of a real SAR image with equivalent number of looks 4.5. The equivalent number of looks is an estimated value over correlated observations from real data. To evaluate the filter efficiency related to speckle strength reduction, we have used the estimated standard deviation to the mean ratio $(\hat{\sigma}_z)$, which is shown in Fig. 5(b).

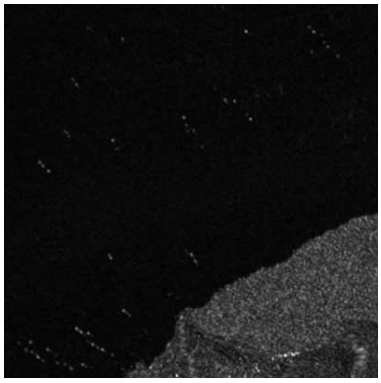

(a)

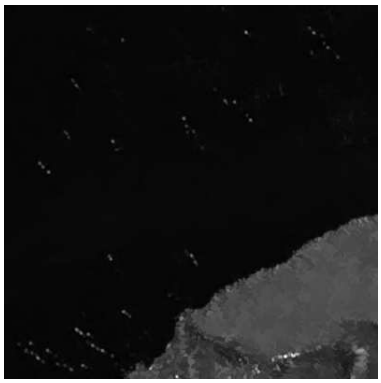

(b)

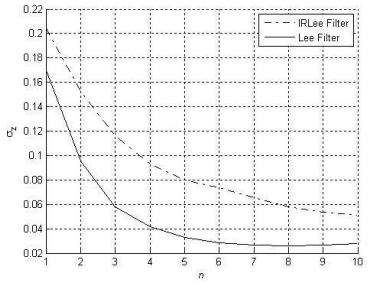

(c)

Fig. 5. Proposed filtering algorithm applied to SAR image with equivalent number of looks 4.5. (a) Original image (b) filtering result and (c) $(\hat{\sigma}_z)$ evaluated in the several iterations.

V. Conclusions

We have presented three different approaches for SAR image processing applications with the purpose of preserving

targets. These techniques incorporate speckle noise statistics in its design and furthermore they present two main advantages: No preprocessing or postprocessing requirements to track targets in noisy images and low sensitivity to multiplicative noise.

Segmentation tasks in SAR image applications (e.g. point target detection) can be complicated due to the granular appearance of SAR images. Nevertheless, we approach and overcome this difficulty by presenting a segmentation algorithm for target detection without prior speckle filtering. The segmentation results outlined an interesting and promising approach which confirm that segmentation algorithms driven by speckle statistics perform well in SAR images.

Regarding the compression application, we have presented promising results, considering real SAR images. We can observed the SPIHT performance related to fine detail preservation can be improved without changing the bit rate significantly.

When speckle filtering is required, it is expected that an ideal speckle filter should reduce noise while preserving edges and fine details. The standard Lee's filter can reduce speckle effects but it also smears edges. The $IRLee$ algorithm is effective in reducing speckle noise from uniform areas and in enhancing and preserving edges, enabling larger windows to be used, with consequent lower impact on edges and targets.

The other experiments included images contaminated by speckle noise, following square root of gamma distributions. The results pointed that the methods are appropriate for point target detection in several applications.

Further developments should include the processing of size-independent targets such as military tanks, archaeological sites, ice floe, buoys for oceanographic studies and different clutter backgrounds.

REFERENCES

[1] S. P. Luttrell and C. J. Oliver, "Prior knowledge in synthetic-aperture radar processing," *J. Phys. D: Appl. Phys.*, vol. 19, pp. 333–356, 1986.

[2] R. C. P. Marques, F. N. S. Medeiros, and D. M. Ushizima, "Target detection in SAR images based on a level set approach," *IEEE Trans. on Syst., Man and Cybern. C, Appl. and Rev.*, vol. 39, no. 2, pp. 214–222, March 2009.

[3] J. S. Lee, "Speckle analysis and smoothing of synthetic aperture radar images," *Comput. Graphics and Image Process.*, vol. 17, pp. 24–32, 1981.

[4] J. A. Sethian, *Level Set Methods and Fast Mar.ing Methos: Evolving Interfaces in Computational Geometry, Fluid Mechanics, Comput. Vision and Materials Science*. Cambridge: Cambridge University Press, 1998.

[5] J. M. Park, W. J. Song, and W. A. Pearlman, "Speckle filtering of SAR images based on adaptive windowing," *IEE Proc. Vision,Image and Signal Process.*, vol. 146, no. 33, pp. 191–197, 1999.

[6] R. C. P. Marques, D. S. Ferreira, F. N. S. Medeiros, J. V. Cruz, and M. H. V. Duarte, "SAR image compression using bounded variation component analysis," in *Proceedings of SIBGRAPI 2008*, Campo Grande, 2008.

[7] L. A. Vese and S. J. Osher, "Image denoising and decomposition with total variation minimization and oscillatory functions," *Journal of Mathematical Imaging and Vision*, vol. 20, no. 1-2, pp. 7–18, March 2004.

[8] A. Said and W. Pearlman, "A new, fast, and efficient image codec based on set partitioning in hierarchical trees," *IEEE Trans. Circuits Syst. Video Technol.*, vol. 6, pp. 243–250, June 1996.

[9] C. I. O. Martins, F. N. S. Medeiros, D. M. Ushizima, F. N. Bezerra, R. C. P. Marques, and N. D. D. Mascarenhas, "Iterative self-dual reconstruction on radar image recovery," in *IEEE Workshop on Applications of Computer Vision (WACV)*, Snowbird, Utah, 2009, pp. 37–42.

[10] J. P. Serra, *Image Analysis and Mathematical Morphology*, 2nd ed. Orlando: Academic Press, 1988, vol. 2.

[11] J. S. Lee, "Refined filtering of image noise using local statistics," *Comput. Graphics and Image Process*, no. 15, pp. 380–389, 1981.

[12] I. B. Ayed, A. Mitiche, and Z. Belhadj, "Multiregion level-set partitioning of synthetic aperture radar images," *IEEE Trans. Pattern Anal. Mach. Intell.*, vol. 27, no. 5, pp. 793–800, May 2005.

[13] J.-F. Aujol, G. Aubert, L. Blancc-Feraud, and A. Chambolle, "Image decomposition application to SAR images," *Lecture Notes in Computing Science*, no. 2695, pp. 297–312, 2003.

[14] Z. Zeng and I. G. Cumming, "SAR image data compression using a tree-structure wavelet transform," *IEEE Trans. on Geoscience and Remote Sensing*, vol. 39, no. 3, pp. 546–552, March 2001.

[15] M. Sun and C. Li, "A new complex SAR image compression quality metric," in *Proc. of IGARSS 2005*, vol. 7, 2005, pp. 4697–4700.

[16] A. Achim, P. Tsakalides, and A. Bezerianos, "SAR image denoising via bayesian wavelet shrinkage based on heavy-tailed modeling," *IEEE Trans. Geosci. Remote Sens.*, vol. 41, no. 8, pp. 1773–1784, Aug. 2003.

[17] F. Sattar, L. Floreby, G. Salomonsson, and B. Lövström, "Image enhancement based on a nonlinear multiscale method," *IEEE Trans. on Image Process.*, vol. 6, no. 6, pp. 888–895, Jun. 1997.